Ninth Canadian Conference on
Earthquake Engineering
Ottawa, Ontario, Canada
26-29 June 2007

CYCLIC BEHAVIOR OF FIBER-REINFORCED PLASTERBOARD WITH CORE CONCRETE COMPOSITE SHEAR WALLS

X. Jiang[1] and Y. Gu[2]

ABSTRACT

This paper presents the results of an experimental research program concerned with the response of fiber-reinforced plasterboard filled with core concrete under cyclic loading. First of all the paper offers information pertinent to the experimental work, including a description of the test rig, instrumentation of the specimens, control procedure of the test, detail of model manufacture, properties of materials used and the loading regime. The description of the experiments together with the loading procedure and the crack development is shown subsequently. Based on these experiments, this paper then inquires into the capacity of shearing force, the damage state, the ductility features, and the hysteretic characteristics, etc. The result of the test indicates that under the action of the horizontal cyclic load and vertical load, the fiber-reinforced plasterboard and core concrete work together to resist load effects, and the capacity of this composite is of satisfactory seismic-resistant behavior.

Introduction

With the prohibition against use of the clay bricks, it is so urgent to study new building system and new walling materials in China. Nowadays the conception of ecological buildings and environment protection materials are well accepted by people. The construction material mainly made of gypsum attracts the attention of the building industry. In the past, gypsum products were only used as partition walls, furred ceilings and so on. Recently a new kind of gypsum walling product has been developed and produced, which is 120mm thick, light weight, hollow-core and fiber-reinforced plasterboard. Many buildings have been constructed with such panels in Australia.

The fiber-reinforced plasterboard, which inside cavities are filled with the reinforced concrete, is regarded as a vertical and horizontal wall-bearing structure. China’s 33 percent of her territory is located in seismic regions, where seismic fortification intensity is predicted to be over 7 degrees. Buildings constructed there must employ seismic design and need some seismic fortification measures. In order to meet the need of projects in China, appropriate new arrangements should be made for such panel. In this paper, two test specimens of fiber-reinforced plasterboards with core concrete were designed to show whether this kind of composite walls could be used as a load-bearing wall in seismic regions.

[1]Professor, Dept. of Civil Engineering, Tianjin University, 92 Weijin Road, Naikai District, Tianjin, 300072. E-mail: jiangxinliang@126.com
[2]Doctoral Graduate Student, Dept. of Civil Engineering, Tianjin University, 92 Weijin Road, Naikai District, Tianjin, 300072. E-mail:gu_yanyan@126.com

Objective of the Study

The main objective of the research is to conduct cyclic-test of two specimens and collect the response of the fiber-reinforced plasterboard with core concrete subjected to horizontal cyclic loading with constant vertical loading. Report some of the important behavior aspects and provide technical support for the use and wide application of such panels in China.

Experimental Programs

Two specimens, hereafter referred to as SW1 and SW2, were constructed at scale 1:1. The two walls, considered to represent the critical story element of a structural wall system with a rectangular cross-section, were tested until their failure after the cyclic horizontal loadings.

Wall Details

The two tested composite walls, which consisted of fiber-reinforced plasterboard and reinforced core concrete, were 2700mm high, 1520mm wide, and 120mm thick. In both cases they were monolithically connected to an upper and lower beam. The former functioned both as the element through which vertical and horizontal loads were applied to the walls, and as a cage for anchoring the vertical bars, while the latter was utilized to clamp down the specimen to the laboratory floor, simulating a rigid foundation.

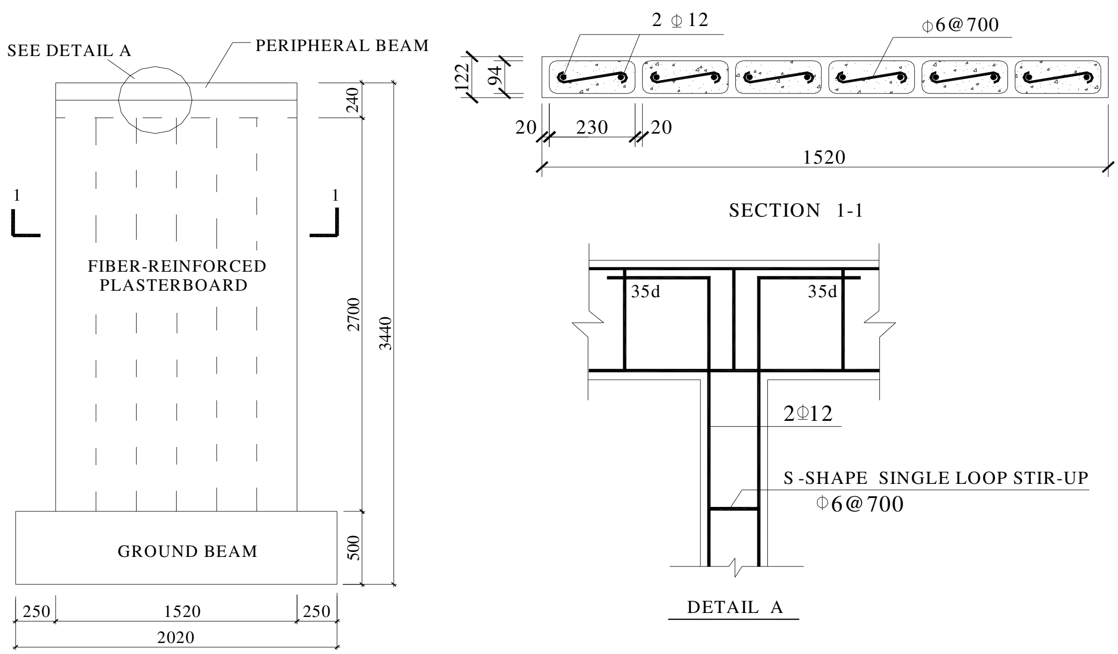

Figure 1. Elevation and details of specimens.

The nominal dimensions of the specimens, together with the arrangement of the vertical reinforcement, are shown in Fig.1. The vertical reinforcement comprised indented bars 12mm in diameter, 2 at each cavity. High-tensile indented bars 6mm in diameter were used as a S-shape single loop stir-up to fix the vertical reinforcement. The yield f_y and ultimate strength f_u characteristics of the steel bars used are summarized in Table 1.

Normal weight concrete for the two specimens was batched by a local ready-mix concrete supplier. The mix of a maximum aggregate size of 10mm and cement content of about 298kg/m^3 was used in SW1, 370kg/m^3 in SW2. The two specimens were cast at the same day, while core concrete test cubes, square columns and modulus were cast. Specified 28-day compressive cube strength was 32.42N/mm^2 for SW1 and 43.78N/mm^2 for SW2. The compressive strength and the tensile strength of the fiber-reinforced plasterboard tested in the laboratory were 5.17N/mm^2 and 2.95N/mm^2 respectively.

Table 1. Properties of reinforcing bars

Type	Yield strength f_y, N/mm^2	Ultimate strength f_u, N/mm^2
12mm indented bars	408.2	616
6mm high-tensile indented bars	491	644

Test Setup

The setup of the testing arrangements, including vertical loading system and horizontal loading system, is shown in Fig.2.

Vertical Loading System

A stiff steel I-shape beam was hung and fixed on two longitudinal beams which were fixed between portal frames in the laboratory. Six hydraulic jacks, which could provide 300kN of pressure, were placed on the I-shape beam. Vertical load was applied to the peripheral beam through the six hydraulic jacks. To eliminate the friction between the jacks and the specimen, load was applied through solid circular rollers, which were encased in a stiff rectangular box. The center of the jack should be on the axis of the beam to ensure axial pressure on the composite wall.

Horizontal Loading System

The actuator, which could provide ±500kN of maximum push-pull force and 300mm of maximum displacement, was fixed to the R/C reaction wall that was in turn fixed to the laboratory floor. The horizontal load was applied through the peripheral beam to spread cyclic forces and displacement on the specimen.

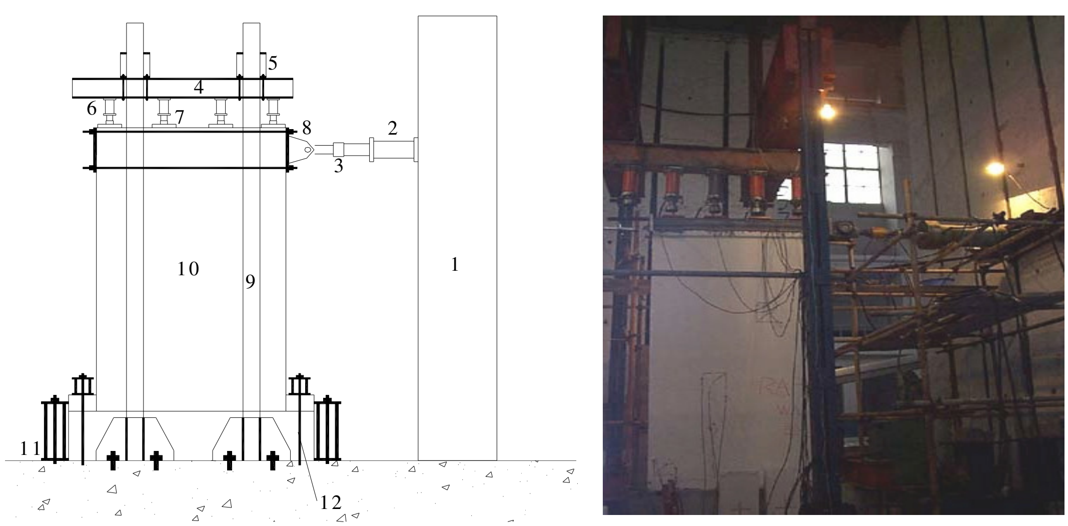

1.R/C reaction wall; 2.actuator; 3.load cell; 4.beam bearing vertical load;
5.longitudinal beam between portal frame; 6.vertical hydraulic jack; 7.roller;
8.steel tie bar; 9.portal frame; 10.test specimen; 11.reaction steel beam; 12.anchor bolts

Figure 2. Test setup.

Instrumentation, Loading History and Test Procedure

Linear variable displacement transducers (LVDTs) were put on the specimens to measure the displacement of points interested on the specimens, as shown in Fig.3. LVDT1 was placed on the center line of the top beam, LVDT2 was placed on the center line by half height of the ground beam and used to eliminate the effect of the ground beam drifting in the test. LVDT1 and LVDT2 composed a loop to measure the relative displacement of the composite wall. The hysteretic curve was recorded by the X-Y functional recorder and drawn directly by a computer.

A severe cyclic loading regime was used. Before the specimen cracking, load control was used. At each new load level, one full cycle was imposed, the load level having been increased by 20kN until the specimen was cracked. When the specimen reached the crack load, displacement control was used. At each new displacement level, the increment of the displacement was half or one time as big as that of the cracking displacement. The two specimens were tested to failure.

In each test, first the specimen was hoisted and located on the right site, then tightened on the laboratory floor. The actuator monitoring system and all instruments were connected and calibrated. Later a warm-up test was carried out in which a very small amount of cyclic actuator load was employed to check the performance of the actuator and all instruments. After that, the real test began. The actuator applied lateral loads and displacements to the top of the specimen in preplanned regime. At each increment, the load was remained constant for at least 2 minute to measure the load and deformation response of the specimens, mark the cracks formed during every cycle at every maximum load or displacement level, and take photographs of the crack. The actuator continued applying load and displacement cycles until the specimen was failed.

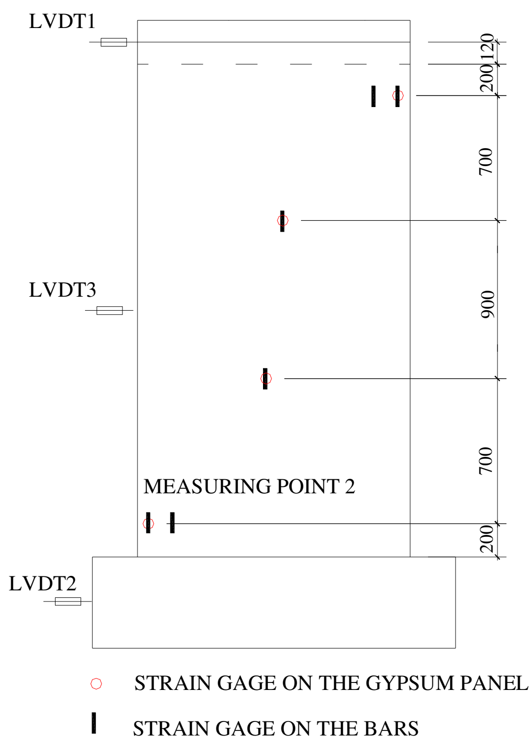

Figure 3. Location of test points.

Test Results and Discussion

The main results of the tests are given in Table 2 and Fig.4. Table 2 provides information related to principal results of the specimens tested in the program. P_{cr}, P_u and P are presented the crack load, ultimate load and failure load respectively, while Δ_{cr}, Δ_u and Δ are presented the displacement corresponding with the above-mentioned loads. Fig.4 depicts the horizontal load-top displacement curve established in the tests.

Table 2. Main test results.

Specimen	Crack		Ultimate		Failure	
	Load P_{cr} /kN	**Displacement Δ_{cr} /mm**	**Load P_u /kN**	**Displacement Δ_u /mm**	**Load P /kN**	**Displacement Δ /mm**
SW1	85	4.86	169	26.86	140	75.7
SW2	93	4.16	161	17.2	133	41.35

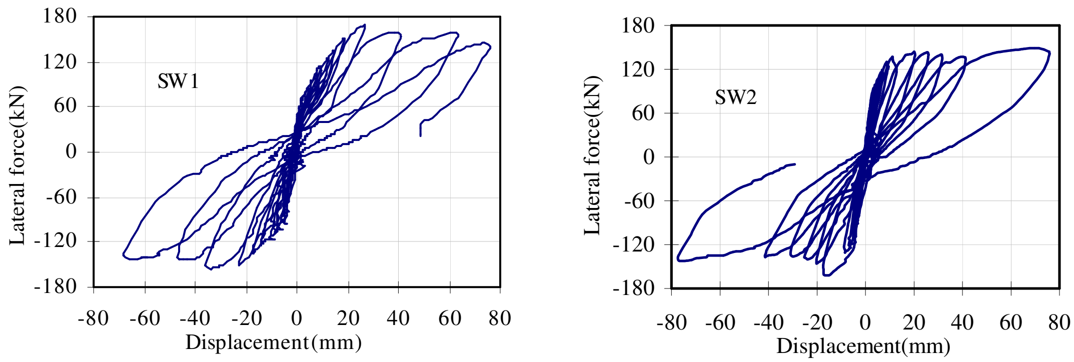

Figure 4. Hysteretic loops of specimens.

Cracking Process and Failure Mode

The cracking process of SW1 and SW2 was similar, both of which all included stages of elasticity, cracking development and failure. Here only the SW1 was used to illustrate the cracking process and the failure mode.

The top displacement of the specimen was very small and the hysteretic curve of load-displacement was approximate to line at the initial applying load, thus the specimen was regarded as working in an elastic state. Two horizontal cracks initially appeared near the middle-lower part of the tensile zone of plasterboard, as shown in Fig. 5(a), when around 50 percent of the ultimate load was reached. At the horizontal load approached 60 percent of its maximum value, several parallel and short inclined cracks began to appear in the middle of the gypsum panel and from bottom upward, as shown in Fig. 5(b). During consecutive load reversals, new inclined cracks appeared, those existed cracks were developing and propagating. These cracks formed an orthogonal crisscrossing crack pattern on the panel, as Fig. 5(c) demonstrated. When the horizontal load reached the ultimate load, compression crushing crack initially appeared along the height of the wall, and developed with the displacement increasing. Compression crushing crack became a longitudinal crack from bottom to top along the wall height when the top displacement reached its maximum value. At this point the horizontal load descended to 85 percent of the ultimate load and the specimen failed. This failure mode is shown in Fig. 5(d).

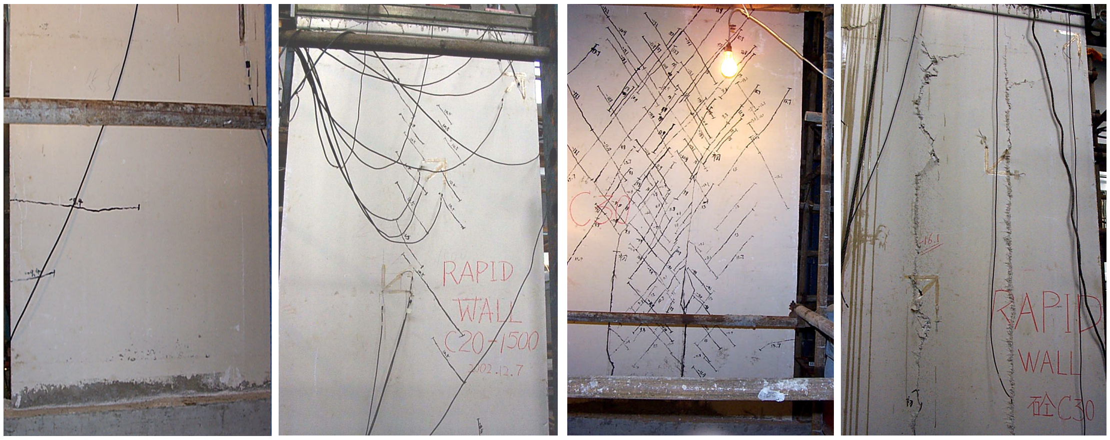

(a) hor. Load=85kN (b) hor. Load=105kN (c) hor. Load=169kN (d) Typical mode of failure

Figure 5. Cracking process and failure mode.

Hysteretic Character

The horizontal load-top horizontal displacement curves of walls SW1 and SW2 are shown in Fig.4 respectively, which indicate a distinctly nonlinear deformational response for the two walls. The specimen was almost elastic before its cracking. The hysteretic loops were small and similar to a line. When the specimen was subjected to the crack load, about 50~60 percent of shear force capacity, the hysteretic curve deviated a little, the area surrounded by the hysteretic loop increased, and the residual deformation initially appeared. This point indicated that the composite panel was performing in inelastic state. After reaching the ultimate load, the horizontal load descended a little while the top horizontal displacement increased quickly for the subsequent cycles. Moderate pinch shown on the hysteretic loops demonstrates the influence of drift which included the bond-slip of the indented bar in core concrete and the slip produced by crack opening and closing. When the horizontal load dropped to less than 85 percent of the ultimate load, the specimen was considered as failed. This point was designated as the point of the maximum ductility.

Strength, Deformation and Stiffness Character

Table 2 indicates the horizontal load-carrying capacity of the specimens. The vertical load of SW2 was larger than that of SW1 and the crack load of SW2 is higher than that of SW1, whereas the crack displacement of SW2 is a little smaller than that of SW1. The ultimate load and corresponding displacement of SW2 are both smaller than those of SW1. Thus it could be seen that too large vertical load would restrict the load-carrying capacity and deformation property.

The variation of the secant stiffness with horizontal displacement of the specimens was illustrated in Fig.6. It indicates that the composite wall stiffness decreases to 75 percent of the initial point tangent stiffness for SW1, 65 percent for SW2 at the initiation of visible cracking level, and at the ultimate level, its value drops to only 26 percent of initial point tangent stiffness for SW1, 16 percent for SW2. For the two specimens subjected to the cyclic load, increasing the displacement of the loading cycles increased their stiffness deterioration.

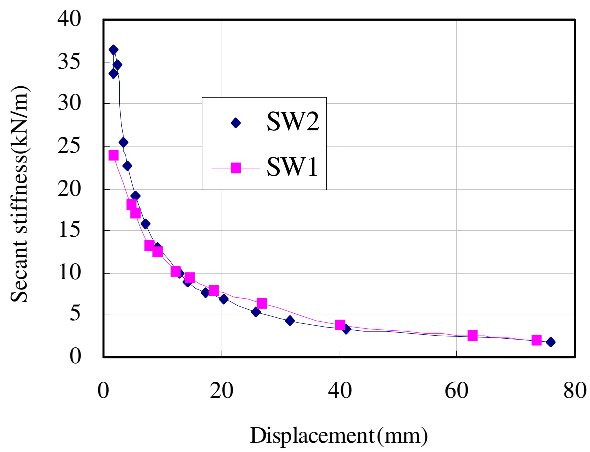

Figure 6. Variation of secant stiffness with horizontal displacement.

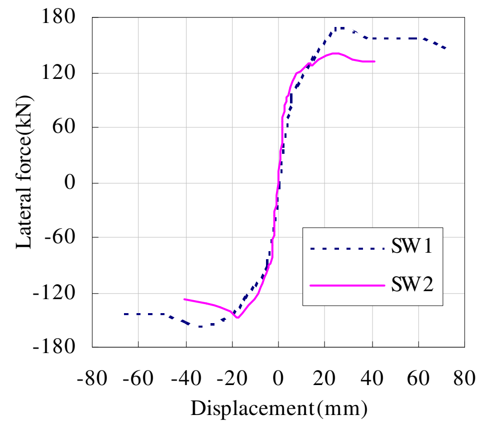

Figure 7. Skeleton curve of specimens.

Skeleton Curve and Ductility

When the peak points of each cycle in the hysteretic curve were connected, skeleton curve of the specimen was formed, as shown in Fig.7. Because the skeleton curve was smooth, general yield moment method was used to define yield load and displacement of the specimen. The ductility presented by μ was the ratio of failure displacement to yield displacement, as shown in Table 3. The ductility of SW1 and SW2 is 8.9 and 6.4 respectively.

Table 3. Ductility of walls.

Specimen	**Yield load (kN)**	**Yield displacement (mm)**	**Failure displacement (mm)**	μ
SW1	108	8.5	75.7	8.9
SW2	112	6.5	41.35	6.4

Strain Measurement

Readings of the strain gage of measuring point 2 assigned in Fig.3 are presented in Fig. 8. The strain of vertical reinforcement and plasterboard are almost coincident with the load-strain curve when the specimen was subjected to the compression force, which indicate that the crack's opening and closing did not affect the stress transfer between the reinforced bar, concrete and plasterboard. When the specimen was subjected to the pulling force, the strain of reinforcement and plasterboard kept identical before cracking. Distinct change appeared on the strain of reinforcement and plasterboard; furthermore the stain of the plasterboard lagged behind the reinforcement after cracking. This phenomenon implied that the tensile force was mainly undertaken by reinforcement and plasterboard before cracking; and after cracking, the incremental force was held by reinforcement.

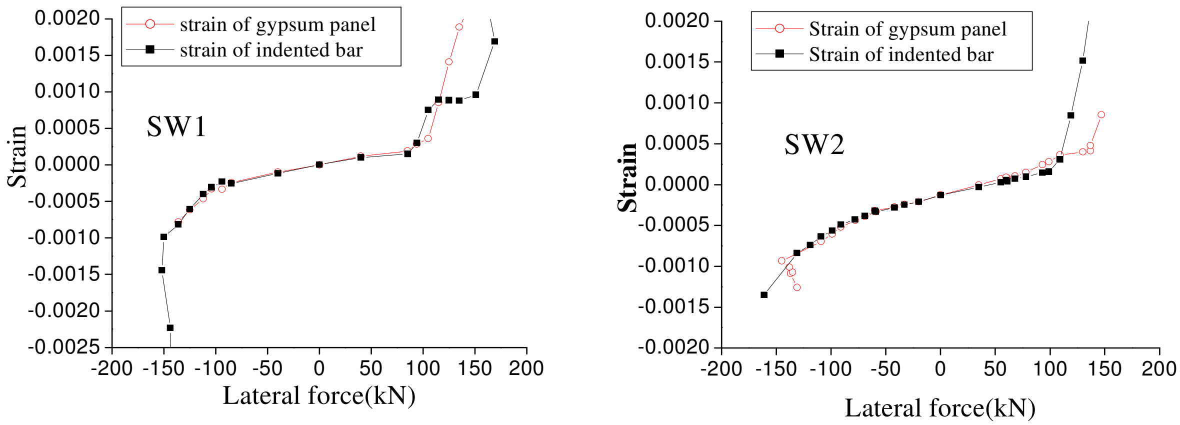

Figure 8. Lateral force-strain curves at measuring point 2.

Conclusions

The results of tests presented above show that the fiber-reinforced plasterboard and core concrete worked together to resist the shear force until the composite wall failed. Fiber-reinforced plasterboard was regarded as the energy-dissipating component. When the composite wall was failed, the cracks were dispersed fully on the gypsum panel and depleted the earthquake energy. This composite wall had a good ductility and seismic-resistant behavior, and could be used in the construction of tier building in future.

Acknowledgments

This project is supported by Tianjin House Construction Development Group Co., LTD. The gypsum panel was provided by Rapid Building Systems Ltd. Liu Kang, Huan Xiaolin and Zheng Shuhai, formerly graduated students at Tianjin University, provided valuable help in preparing specimens and conducting tests. The resources and staff of the laboratory of civil engineering at Tianjin University are very much appreciated. Without their help, this experiment would not have been completed.

References

Industry Criterion of the People's Republic of China, 1997. *Specification of Testing Methods for Earthquake Resistant Building, JGJ 101-96*, Publisher of Building Industry, Beijing, China

Kypros Pilakoutas and Amr Elnashai, 1995. Cyclic Behavior of Reinforced Concrete Cantilever Walls, Part I:Experimental Results, *ACI Structural Journal*, 92(3),271-281.

Liu Li, Li Hongnan and Zhang Jingwei, 2002. Analysis on Aseismic Behavior of Insulation Cavity Energy-Saving Walls, *Earthquake Engineering And Engineering Vibration*, 22(1), 79-84

Loannis D. Lefas and Micheal D. Kotaovos, 1990. Strength and Deformation Characteristics of Reinforced Concrete Walls under Load Reversals, *ACI Structural Journal*, 87(6), 716-726

Quan Chenghua and Tang Daixin, 2002. Experimental Research on Shear Performance of Reinforced Masonry Shear Walls of High Strength Concrete Blocks, *Journal of Building Structures* , 23(2), 79-86

Yu-Fei Wu and Mike P. Dare, 2004. Axial and Shear Behavior of Glass Fiber Reinforced Gypsum Wall Panels:Tests, *Journal of Composites for Construction*, 8(6), 569-578

Zhai Ximei and Tang Daixin, 2001. Restoring Force of Small Concrete Hollow Block Cavity Wall, *Journal of Harbin University of C.E.& Architecture*, 34(6), 26-31

Zhu Bolong, 1989. *Seimic Test for Structures*, Pubulisher of Earthquake, Beijing, China